Simulations of supercooled liquids through swap Monte Carlo

Bonné, Gilles E.

Award date:
2019

EINDHOVEN UNIVERSITY OF TECHNOLOGY

Department of Applied Physics
Theory of Polymers and Soft Matter

Simulations of supercooled liquids through swap Monte Carlo

Bachelor Final Project

G.E. Bonné

Supervisors: dr. L.M.C. Janssen
S. Ciarella MSc
C. Luo MSc

Eindhoven, July 2019

Abstract

Glass formation remains one of the deepest problems in physics. The cooling of a supercooled liquid causes an extreme slowdown in dynamics, due to a dramatic increase in viscosity. This is the basic idea of the glass transition. The problem is that experiments and simulations are limited by this increase in viscosity, thus we need to surpass this limit to solve the glass transition problem. This work looks into a recently proposed simulation technique to increase the domain of glass transition studies able to be explored. The simulation technique builds on top of conventional Monte Carlo molecular modeling methods by introducing particle swaps. The efficiency of these particle swaps in a high-density mixture is strongly decreased for large particle diameter differences, therefore a continuous size distribution (or continuous polydispersity) is used. The continuous size distribution allows us to harness the power of the particle swap moves, which is presented to be a speedup in dynamics of at least an order of magnitude. Furthermore, a discrete polydisperse mixture is introduced to approximate the structure and the speedup in dynamics of the continuous polydisperse mixture. It is found that for a system of 10 components the speedup in dynamics is approximately equal to the speedup from a continuous polydisperse mixture, while 20 components are needed to have a structure which is very similar to the structure of a continuous polydisperse mixture.

Contents

Chapter 1

Introduction

The theory of the nature of glass ranks among the deepest unsolved problems in condensed matter physics [1]. When quenching a supercooled liquid a very strong slowdown of dynamics happens with only tiny differences in structure. The extreme slowdown of dynamics is captured by an increase in viscosity. The viscosity is defined as to what degree a fluid flows due to internal friction. When the viscosity of this material exceeds 10^{13} kg $m^{-1}s^{-1}$ it is defined to be a glass [2]. Glass has the macroscopic properties, namely rigidity, of a solid, while on a microscopic scale it appears to be disordered, like a liquid. Figure 1.1 shows a schematic view of the structure and dynamics of a liquid and a glass. The structure of a liquid and a glass look nearly identical. In contrast, the dynamics look entirely different. For a liquid all the particles can diffuse fast through the system, while for a glass this diffusion is very slow.

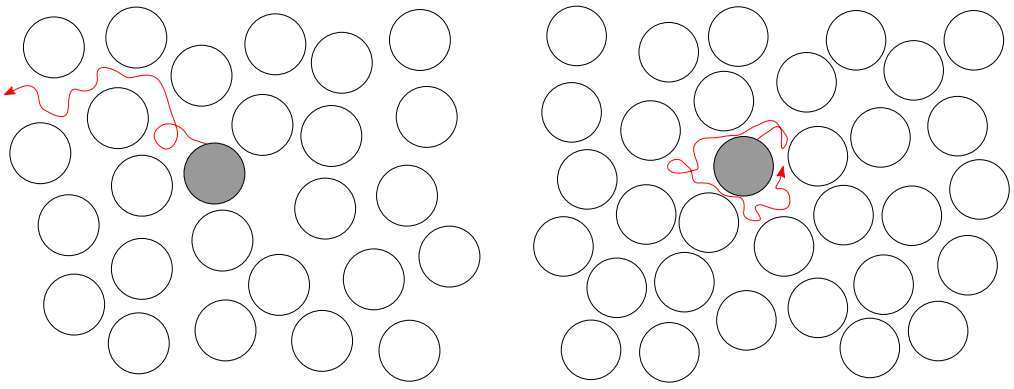

(a) Liquid. (b) Glass.

Figure 1.1: Schematic view of a material in the liquid and in the glass state. The red line represents the particle trajectory. Adapted from [3].

To study the dynamics around the glass transition one can use molecular simulations. Conventional techniques use either Monte Carlo methods or Molecular Dynamics simulations. Monte Carlo methods randomly sample states according to Boltzmann probabilities, while Molecular Dynamics describes the dynamics by solving Newton's equations of motion [4]. These simulations are only able to simulate 5 orders of magnitude of the slowing down of dynamics approaching the glass transition, while 13 orders of magnitudes of slowdown have been shown in experiments [5].

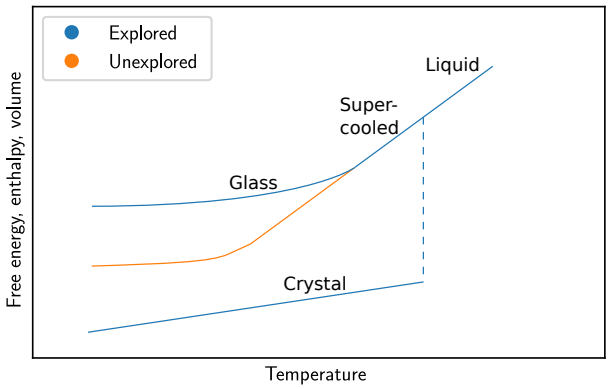

Figure 1.2: Sketch of the free energy, enthalpy or volume as function of the temperature showing the current temperature region that is able to be studied and how this region can expand using new simulation protocols. Adapted from Royall et al. [6].

When supercooling a liquid the viscosity increases. At some point the system becomes so viscous that is solid on experimental timescales [6]. This corresponds to the system falling out of equilibrium into a non-ergodic glass phase. Different simulation protocols can allow us to reach equilibrium for lower temperature supercooled liquids without falling out of equilibrium, to explore the deeply supercooled liquid region where new physics could appear. This is visualized in figure 1.2. In this work a new type of Monte Carlo simulation is used which makes it possible to study a part of the previously inaccessible area.

Grigera and Parisi [7] introduced the use of particle swaps in addition to traditional translation Monte Carlo moves. This technique makes it possible that particles can more easily break out of the cage formed by other particles. Normally, a lot of particles have to move to make it possible for two particles to switch positions. Ninarello et al. [5] studied a nonadditive continuous polydisperse system interaction with a soft repulsive pair potential and claimed to have a thermalization speedup of around 10 orders of magnitude. In this work an effort is made to

show the effect of swap Monte Carlo moves on the dynamics and the structure of a supercooled liquid

Mode-Coupling Theory (MCT) is a theory developed to describe the dynamics of glass formation from the structure. MCT becomes increasingly difficult when increasing the number of components. The mixture studied by Ninarello et al. [5] has an infinite amount of components which makes MCT extremely difficult, if not impossible [8]. It is, therefore, paramount that the number of components is reduced to work with existing theories of glass formation. Therefore, the second research question goes into transforming this continuous polydisperse mixture to a discrete polydisperse mixture by asking:

how many species should a system contain to have similar dynamics and structure as a continuous polydisperse system?

In chapter 2 Monte Carlo molecular modeling is discussed for both the conventional translation moves as well as the recently introduced swap moves. In addition, the interaction between particles, the size distribution and the implementation of the simulation is explained. Consequently, in chapter 3 the observables of interest, equilibration and the verification of the simulation is presented. The results and discussion for a continuous polydisperse mixture and for the finite multicomponent mixture are given in chapter 4 and 5.

Chapter 2

Simulation

Consider a system with N spheres, a volumetric number density ρ and a temperature T. The volumetric number density describes the concentration of spheres in three-dimensional space and is defined as

$$\rho = \frac{N}{V}, \tag{2.1}$$

where V is the closed cubic volume. As a result of this, the system is a canonical ensemble with configuration $\mathbf{Q} = (\boldsymbol{q}_1, \boldsymbol{q}_2, ..., \boldsymbol{q}_N)$. This configuration space $\boldsymbol{Q}$ is spanned by vectors pointing in four-dimensional Euclidean space

$$\boldsymbol{q}_i = \begin{pmatrix} x_i \\ y_i \\ z_i \\ R_i \end{pmatrix} = \begin{pmatrix} \boldsymbol{r}_i \\ R_i \end{pmatrix}, \tag{2.2}$$

for $i = 1, 2, ..., N$ where x_i, y_i and z_i represent the position in a three-dimensional Cartesian coordinate system also denoted with the vector $\boldsymbol{r}_i$ and R_i the radius of the sphere. The radii R_i are included in the configuration as these radii are not fixed when including the recently introduced swap moves.

To simulate the states of the system a technique from statistical mechanics called Monte Carlo molecular modeling is used. Monte Carlo simulations randomly sample the states of a system according to Boltzmann probabilities. The Monte Carlo simulations are Markovian by nature, which means that the next state is computed by only using the previous state of the system. For the specific implementation of the Monte Carlo technique, the Metropolis [9] algorithm is applied to the problem.

2.1 Monte Carlo

In the canonical ensemble the thermal average for some observable A is given by

$$\langle A(\boldsymbol{Q}) \rangle_T = \frac{1}{Z} \int A(\boldsymbol{Q}) \exp\left(-\frac{E}{k_b T}\right) d\boldsymbol{Q}, \tag{2.3}$$

where the partition function is mathematically state by

$$Z = \int \exp\left(-\frac{E}{k_b T}\right) d\boldsymbol{Q}, \tag{2.4}$$

where E is the energy and k_b is the Boltzmann constant [10]. To approximate equation 2.3 by a summation over all possible configurations $\{\boldsymbol{Q}_1, \boldsymbol{Q}_2, ..., \boldsymbol{Q}_M\}$, where M is the total

number of configurations, then for $M \to \infty$ the average of the observable

$$\overline{A(\boldsymbol{Q})} = \frac{\sum_{l=1}^{M} \exp\left(-\frac{E(\boldsymbol{Q}_l)}{k_B T} A(\boldsymbol{Q}_l)\right)}{\sum_{l=1}^{M} \exp\left(-\frac{E(\boldsymbol{Q}_l)}{k_B T}\right)}. \tag{2.5}$$

By implementing numerical integration schemes one needs to do the summations in equation 2.5 over all possible states of the system far exceeding current computational capabilities. When choosing the points at which is sampled randomly according to some probability function rather than a regular grid, it is possible to work with a small subset of these states [10]. By sampling according to some probability function $P(\boldsymbol{Q})$ equation 2.5 converts to

$$\overline{A(\boldsymbol{Q})} = \frac{\sum_{l=1}^{M} \exp\left(-\frac{E(\boldsymbol{Q}_l)}{k_B T} A(\boldsymbol{Q}_l)\right)/P(\boldsymbol{Q}_l)}{\sum_{l=1}^{M} \exp\left(-\frac{E(\boldsymbol{Q}_l)}{k_B T}\right)/P(\boldsymbol{Q}_l)}. \tag{2.6}$$

Using a choice of $P(\boldsymbol{Q}_l) \propto \exp\left(-\frac{E(\boldsymbol{Q}_l)}{k_b T}\right)$ equation 2.6 reduces to

$$\overline{A(\boldsymbol{Q})} = \frac{1}{M} \sum_{l=1}^{M} A(\boldsymbol{Q}_l). \tag{2.7}$$

Metropolis et al. [9] introduced a scheme to make the next state $\boldsymbol{Q'}$ dependent on the previous state $\boldsymbol{Q}$, a so called Markov process, via transition probability $W(\boldsymbol{Q} \to \boldsymbol{Q'})$ [10]. It is possible to find a transition probability W such that for $M \to \infty$ the distribution $P(\boldsymbol{Q})$ moves to the equilibrium distribution

$$P_{eq}(\boldsymbol{Q}) = \frac{1}{Z} \exp\left(-\frac{E(\boldsymbol{Q})}{k_b T}\right), \tag{2.8}$$

by requiring that the condition of detailed balance [10] holds:

$$P_{eq}(\boldsymbol{Q}) W(\boldsymbol{Q} \to \boldsymbol{Q'}) = P_{eq}(\boldsymbol{Q'}) W(\boldsymbol{Q'} \to \boldsymbol{Q}). \tag{2.9}$$

Equation 2.9 shows that

$$\frac{W(\boldsymbol{Q} \to \boldsymbol{Q'})}{W(\boldsymbol{Q'} \to \boldsymbol{Q})} = \exp\left(-\frac{\Delta E}{k_b T}\right) \tag{2.10}$$

only depends on the energy change $\Delta E = E(\boldsymbol{Q'}) - E(\boldsymbol{Q})$ [10]. As equation 2.10 does not provides a exact choice for the transition probability $W(\boldsymbol{Q} \to \boldsymbol{Q'})$, a form of the transition probability suggested by literature [11] is used in this report:

$$W(\boldsymbol{Q} \to \boldsymbol{Q'}) = \min\left[1, \exp\left(-\frac{E(\boldsymbol{Q'}) - E(\boldsymbol{Q})}{k_b T}\right)\right]. \tag{2.11}$$

2.2 The Metropolis algorithm

To make it possible to change states while preserving detailed balance Metropolis et al. [9] proposed the following method:

1. pick a random particle;
2. calculate the energy of the system $E(\boldsymbol{Q})$;
3. propose a random translation to the particle within a cubic box with edge length $2l$ around the particle as visualized in figure 2.1;
4. calculate the energy of the system with the particle in the new position $E(\boldsymbol{Q'})$;
5. accept the move with the acceptance probability given in equation 2.11.

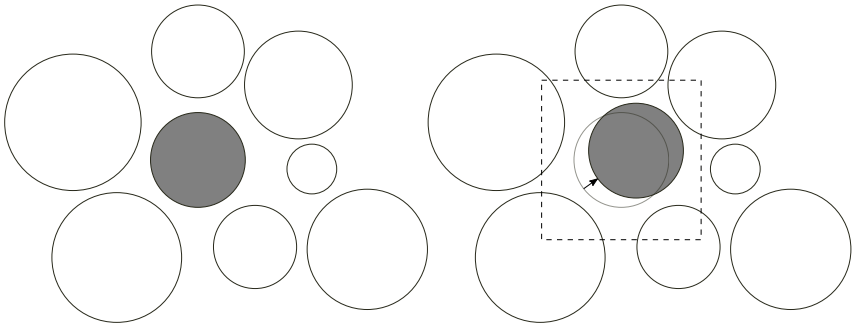

(a) Before translation move. (b) After translation move.

Figure 2.1: Two-dimensional visualization of Monte Carlo translations. The particle indicated in gray is the particle randomly chosen and the dash box, with edge lengths $2l$, depicts the positional constraint for the random translation.

For a system at high densities swapping two particles is a cooperative, thus slow, process [7]. It takes a lot of time for the particles to move around each other as the high density encapsulated the two particles strongly. To solve this problem Grigera and Parisi [7] introduced particle swaps in addition to the traditional Monte Carlo moves. This ensures that the swapping of both particles is made non-cooperative [7]. When the Metropolis algorithm is applied to swap moves the method is defined as:

1. pick two random particles;
2. calculate the energy of the system $E(\boldsymbol{Q})$;
3. propose to swap both particles as visualized in figure 2.2;
4. calculate the energy of the system with both particles in the new configuration $E(\boldsymbol{Q'})$;
5. accept the move with the acceptance probability given in equation 2.11.

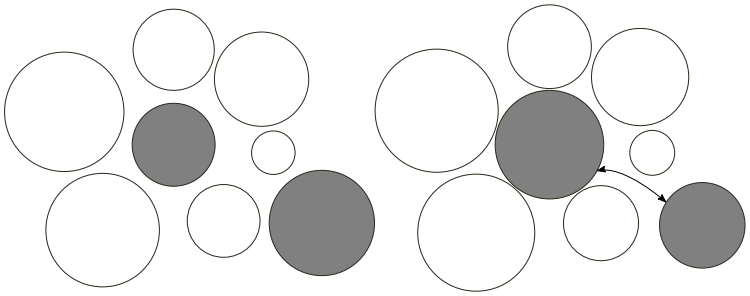

(a) Before swap move. (b) After swap move.

Figure 2.2: Two-dimensional visualization of Monte Carlo swaps. The particles indicated in gray are the particles randomly chosen.

2.3 Computational model

2.3.1 Interaction potential

To study the dynamics of a supercooled liquid of soft spheres a soft repulsive pair interaction potential is used. Following Ninarello et al. [5] the soft repulsive pair (SRP) potential [5]

$$V_{\mathrm{SRP}}(r_{ij}) = \begin{cases} \left(\frac{\sigma_{ij}}{r_{ij}}\right)^n + c_4\left(\frac{r_{ij}}{\sigma_{ij}}\right)^4 + c_2\left(\frac{r_{ij}}{\sigma_{ij}}\right)^2 + c_0 & \text{if } r_{ij} < 1.25\sigma \\ 0 & \text{if } r_{ij} \geq 1.25\sigma, \end{cases} \tag{2.12}$$

where σ_{ij} is the diameter of an hard sphere or otherwise known as the summed Van der Waals radius of particles i and j; r_{ij} is the Euclidean distance between the centers of particle i and j; n is the level of softness of the potential; and the coefficients c_0, c_2 and c_4 are to make the potential, the first and the second derivative continuous at the chosen cut-off distance $r_{\text{cut}} = 1.25\sigma_{ij}$.

By requiring that the derivatives up to the second order are continuous this potential has an advantage over the commonly used repulsive Weeks-Chandler-Anderson (WCA) [12] potential derived in appendix A from the Lennard-Jones potential, which has an attractive as well as a repulsive part. The second derivative of the WCA-potential is not continuous at the cut-off distance, which results in instabilities in the solutions when performing Molecular Dynamics simulations [13].

These requirements mean that

$$V_{\text{SRP}}(r_{ij} = r_{\text{cut}}) = \left.\frac{dV_{\text{SRP}}(r_{ij})}{dr_{ij}}\right|_{r_{ij}=r_{\text{cut}}} = \left.\frac{d^2V_{\text{SRP}}(r_{ij})}{dr_{ij}^2}\right|_{r_{ij}=r_{\text{cut}}} = 0. \tag{2.13}$$

Solving this set of equation for the coefficients gives:

$$c_0 = -2^{-3+2n}5^{-n}(2+n)(4+n), \tag{2.14}$$

$$c_2 = 4^{1+n}5^{-2-n}n(4+n), \tag{2.15}$$

$$c_4 = -2^{5+2n}5^{-4-n}n(2+n) \tag{2.16}$$

which for the case used in this work, a softness parameter of $n = 12$ [5], reduces to $c_0 = -1.92415$, $c_2 = 2.11106$ and $c_4 = -0.591097$. The SRP-potential is visualized in figure 2.3.

The force in the x-direction due to the soft repulsive pair potential

$$F_{\text{SRP}_x}(x, r_{ij}) = \begin{cases} \left[-c_4\dfrac{4r_{ij}^2}{\sigma_{ij}^4} - c_2\dfrac{2}{\sigma_{ij}^2} + \dfrac{n}{r_{ij}^2}\left(\dfrac{\sigma_{ij}}{r_{ij}}\right)^n\right]x & \text{if } r_{ij} < 1.25\sigma_{ij} \\ 0 & \text{if } r_{ij} \geq 1.25\sigma_{ij}, \end{cases} \tag{2.17}$$

where x is the one dimensional distance in the x-direction. Similarly, the force is computed for the y and z-direction.

Following Ninarello et al. [5] the cross diameter

$$\sigma_{ij} = \frac{\sigma_i + \sigma_j}{2}(1 - \alpha|\sigma_i - \sigma_j|), \tag{2.18}$$

is used for the pair interaction to make sure that there is a high structural stability in the simulation, where α is a nonadditivity parameter and σ_i and σ_j are the diameters of particles i and j respectively.

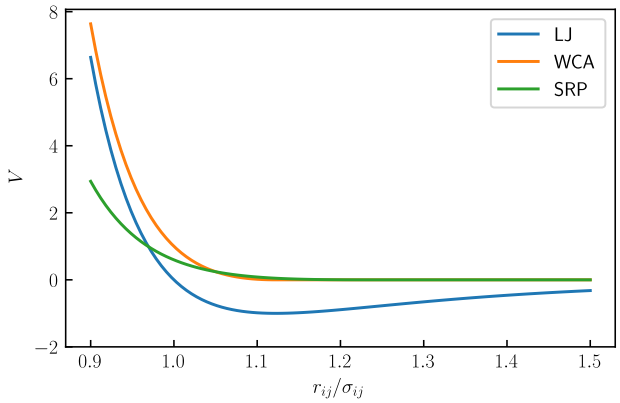

Figure 2.3: Lennard-Jones potential from equation A.1 with $\epsilon = 1$, Weeks-Chandler-Andersen potential following equation A.2 with $\epsilon = 1$ and the soft repulsive pair potential from equation 2.12 with $n = 12$ and $c_0 = -1.92415$, $c_2 = 2.11106$ and $c_4 = -0.591097$.

2.3.2 Particle size distribution

The performance of swap moves for increasing the thermalization is strongly related to the diameter differences of the particles that are swapped. A very small diameter difference in, for example, a binary mixture would be the best for accelerating thermalization, but makes the system susceptible to crystallization [5]. By using a continuous polydisperse system over a large diameter interval, the diameter differences between individual particles do not necessarily have to be large and the system is less likely to crystallize.

To study these continuous and variable degrees of discrete polydisperse systems which have shown to strengthen glass forming ability, following Ninarello et al. [5], the particle size distribution

$$P(\sigma) = \frac{A}{\sigma^3} \tag{2.19}$$

for $\sigma \in [\sigma_{\min}, \sigma_{\max}]$, where A is a normalization constant and $\sigma_{\min}$ and $\sigma_{\max}$ denote the minimum and maximum particle diameter respectively. The ratio $\sigma_{\max}/\sigma_{\min}$ will be an input parameter for the simulation. The unit of length is defined as the average particle size $\langle\sigma\rangle$. So using the fact that equation 2.19 must be normalized and that the length unit is defined as the average particle size $\langle\sigma\rangle$, which is set to unity within the simulation, a system of two equations is created:

$$\begin{cases} \langle 1 \rangle & = 1 \\ \langle \sigma \rangle & = 1. \end{cases} \tag{2.20}$$

By evaluating equation 2.20 for a continuous polydisperse system, indicated by the number of species $N_s = \infty$, the system gets the form:

$$\begin{cases} \int_{\sigma_{\min}}^{\sigma_{\max}} P(\sigma) d\sigma & = 1 \\ \int_{\sigma_{\min}}^{\sigma_{\max}} \sigma P(\sigma) d\sigma & = 1. \end{cases} \tag{2.21}$$

Solving the system of equations 2.21 gives

$$A = \frac{1}{2} + \frac{1}{\sigma_{\max}/\sigma_{\min} - 1}, \tag{2.22}$$

$$\sigma_{\min} = \frac{1 + \sigma_{\max}/\sigma_{\min}}{2\sigma_{\max}/\sigma_{\min}}, \tag{2.23}$$

$$\sigma_{\max} = \frac{1 + \sigma_{\max}/\sigma_{\min}}{2}. \tag{2.24}$$

For the discrete polydisperse system there are a discrete number of species N_s so evaluating equation 2.20:

$$\begin{cases} \sum_{s=1}^{N_s} P(\sigma_s) & = 1 \\ \sum_{s=1}^{N_s} \sigma_s P(\sigma_s) & = 1, \end{cases} \tag{2.25}$$

where the species s, with $s = 1, 2, ..., N_s$, has diameter

$$\sigma_s = \sigma_{\min} + \frac{(\sigma_{\max} - \sigma_{\min})}{N_s - 1}(s - 1). \tag{2.26}$$

The system of equations 2.25 is not analytically solvable for an arbitrary number of species N_s and is, therefore, computed numerically within the simulations.

2.4 Computational details

Due to the nature of Monte Carlo simulations, there is no explicit time involved. The time is therefore given in units of the number of particles N. In practice, this means that the total elapsed time is the total number of attempted Monte Carlo moves divided by the number of particles N.

The system is simulated using periodic boundary conditions which mean that a particle exiting the box on one side it reappears at the opposite side of the box where it exited, as visualized in figure 2.4. Periodic boundary conditions allow one to simulate an infinitely large system. Every particle interacts with all the particles in a box surrounding that particle.

The simulation starts by placing all N spheres with randomly chosen diameter from the particle size distribution 2.19 with a set ratio $\sigma_{\max}/\sigma_{\min}$ in a cubic lattice as visualized in figure 2.5a. This is done by first determining how many particles should be placed along one dimension with the length $L = \sqrt[3]{V}$ where V is the cubic volume calculated from equation 2.1. Another option is to start from a previously equilibrated state, as for example seen in figure 2.5b. After the initialization, the simulations start for a set number of iterations.

Each iteration starts with the choice of Monte Carlo move, to either swap two particles or to translate a single particle. A swap move is chosen with probability P_{swap}, otherwise, a translation move will take place. The swap probability P_{swap} is defined such that when $P_{\text{swap}} = 0$ only translation moves take place and if $P_{\text{swap}} = 1$ only swap moves will be performed.

Following the Metropolis algorithm discussed in chapter 2. If a translation move is chosen for this iteration a single particle is randomly selected. If a swap move is selected two different particles are randomly selected. For a discretized polydispersity the diameter of the two chosen particles has to be different. Allowing the swap of equally sized particle would result in a possible swap of equally sized particles which would not change the structure, dynamics or energy in any way.

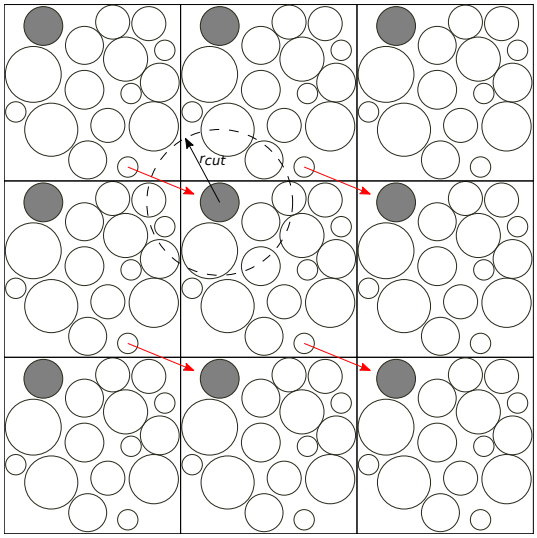

Figure 2.4: Schematic view of periodic boundary conditions and the interaction circle denoted by r_{cut}. The gray particle is indicated in the middle and in the imaginary boxes around the center box. The red arrow indicates how a translation of a particle works when using periodic boundary conditions.

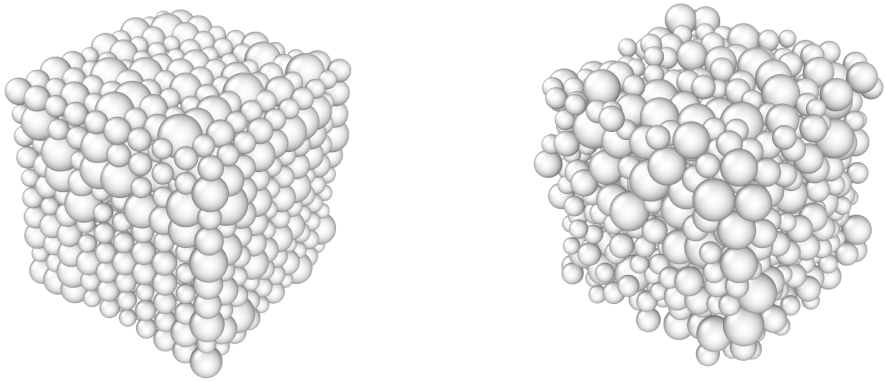

(a) Random initialized lattice.

(b) Equilibrium states at temperature $T = 1$.

Figure 2.5: Graphical visualization of the configuration of $N = 1000$ particles in a box. The diameter shown is the hard sphere diameter σ.

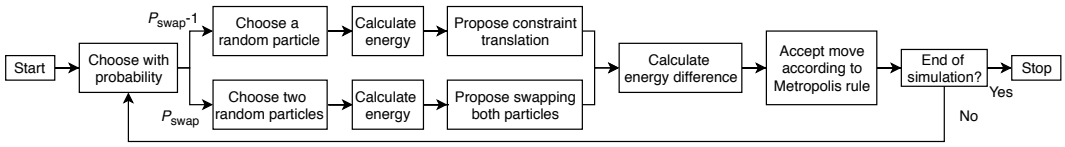

Figure 2.6: Structural outline of the implementation of both the translation and the swap Monte Carlo algorithms.

After the choice of which particle(s) should perform a Monte Carlo move the energy prior to this move is calculated. Instead of calculating the energy of the entire system, the energy is only calculated for all the interactions of the chosen particle or particles with all other particles for translation and swap moves respectively.

For the translation move starting at the initial position $\boldsymbol{r}_i$ the proposed new position is changed with a random translation

$$\boldsymbol{\delta r}_i = \begin{pmatrix} \delta x \\ \delta y \\ \delta z \end{pmatrix}, \tag{2.27}$$

where δx, δy and δz are random perturbations satisfying $\delta x, \delta y, \delta z \in [-l, l]$ with l the maximum translation step size chosen to be 0.1, such that the new position $\boldsymbol{r}_i' = \boldsymbol{r}_i + \boldsymbol{\delta r}_i$. For swap Monte Carlo the proposed move is simply a swap of radii of the two selected particles. This in contrast to the proposed position swap in Grigera and Parisi [7]. By swapping the radii instead of the position the particles perform a sort of random walk in (discretized) diameter space [5].

Then the energy of the proposed move is calculated in the same way as before the move. The probability that the proposed move gets accepted is calculated using equation 2.11 with the energy calculated in both situations.

As for every proposed swap moves the energy has to be calculated for two particles, a useful optimization would be to reject a swap move prior to the energy calculation if the difference between diameter larger than a set value. As seen in figure 4.6, there is an extremely low chance, if not zero, that a move can get accepted for $N_s = 2$ as this would mean swapping $\sigma_{\max}$ and $\sigma_{\min}$.

Aforementioned steps, as summarized in figure 2.6, are repeated for a set number of iterations. The configuration, energy, pressure and Monte Carlo move acceptance ratios are sampled multiple times throughout the full simulation. This allows one to describe the structure, dynamics, Monte Carlo performance and if the system is in equilibrium. The developed simulation code can be found in appendix B.

Within the whole simulation detailed balance is satisfied. Both the Monte Carlo move type and the particle is chosen with a certain probability. By making all choices based upon a probability it ensures that the algorithm is invariant under time reversibility at equilibrium [10].

Chapter 3

Analysis

In this chapter the observables of interest are presented. The observables of interest are the reason why the simulation is created, using these observables one can gain an insight on how the modeled system behaves. Additionally, the methods to determine if a system is in equilibrium are explained. Finally, the simulation code is verified with literature in order to ensure the correctness of the results.

3.1 Observables of interest

To study the behavior of supercooled liquids the structure and dynamics are of interest. For this one needs to track all the particles in space and time. This density in real space

$$\rho(\boldsymbol{r}, t) = \sum_{m=1}^{N} \delta(\boldsymbol{r} - \boldsymbol{r}_m(t)), \tag{3.1}$$

with δ the Dirac delta function. Using a Fourier transform the density modes

$$\rho(\boldsymbol{k}, t) = \sum_{m=1}^{N} e^{i\boldsymbol{k}\cdot\boldsymbol{r}_m(t)}. \tag{3.2}$$

Equation 3.2 allows us to define density-density correlations in the structure over time, which is also known as the collective intermediate scattering function,

$$F_c(\boldsymbol{k}, t) = \frac{1}{N} \left\langle \rho^*(\boldsymbol{k}, 0)\rho(\boldsymbol{k}, t) \right\rangle, \tag{3.3}$$

where ρ^* indicates the complex conjugate of the density modes and $\langle \cdots \rangle$ indicates the ensemble average. By applying equation 3.2 to equation 3.3 gives:

$$F_c(\boldsymbol{k}, t) = \frac{1}{N} \sum_{m=1}^{N} \sum_{n=1}^{N} \left\langle e^{-i\boldsymbol{k}\cdot\boldsymbol{r}_m(0)} e^{i\boldsymbol{k}\cdot\boldsymbol{r}_n(t)} \right\rangle. \tag{3.4}$$

Separating the summation terms in equation 3.4:

$$F_c(\boldsymbol{k}, t) = \frac{1}{N} \left(\sum_{m=1}^{N} \left\langle e^{-i\boldsymbol{k}\cdot\boldsymbol{r}_m(0)} e^{i\boldsymbol{k}\cdot\boldsymbol{r}_m(t)} \right\rangle + \sum_{m=1}^{N} \sum_{\substack{n=1 \\ n\neq m}}^{N} \left\langle e^{-i\boldsymbol{k}\cdot\boldsymbol{r}_m(0)} e^{i\boldsymbol{k}\cdot\boldsymbol{r}_n(t)} \right\rangle \right). \tag{3.5}$$

The first term in equation 3.5 is the correlation of only a particle with itself at a later time. This correlation can be computed separately and will be denoted by the self intermediate

scattering function

$$F_s(\boldsymbol{k}, t) = \frac{1}{N}\left(\sum_{m=1}^{N}\left\langle e^{-i\boldsymbol{k}\cdot\boldsymbol{r}_m(0)} e^{i\boldsymbol{k}\cdot\boldsymbol{r}_m(t)}\right\rangle\right). \tag{3.6}$$

By measuring the intermediate scattering function one can describe the relaxation of a system at the microscopic level [3]. The structural relaxation time τ_α is, by convention, defined as the moment in time that the self intermediate scattering function reaches the value e^{-1}: $F_s(\boldsymbol{k}, \tau_\alpha) = e^{-1}$ [5]. Figure 3.1 shows a sketch of the self intermediate scattering function of equation 3.6 for a liquid, a supercooled liquid and a glass. The self intermediate scattering function for a liquid decorrelates very quickly. For a supercooled liquid there is some plateauing visible before decorrelation. For a glass the self intermediate scattering function does not decay in reasonable timescales [6].

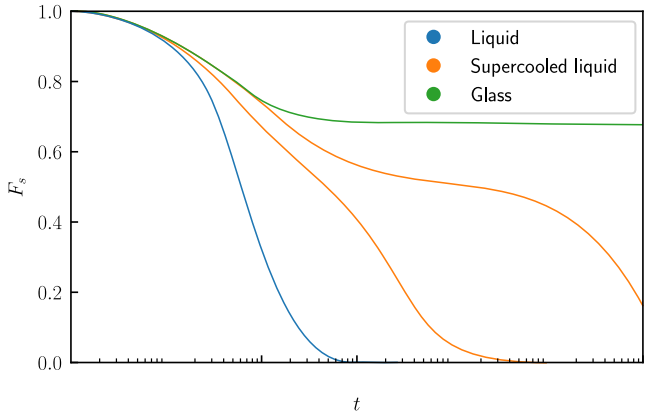

Figure 3.1: Sketch of the self intermediate scattering function over time for a liquid, a supercooled liquid and a glass. Adapted from [3].

By eliminating the time-dependence in equation 3.5 the static structure factor [14]

$$S(\boldsymbol{k}) = \frac{1}{N}\left\langle \sum_{m=1}^{N} e^{i\boldsymbol{k}\cdot\boldsymbol{r}_m} \sum_{n=1}^{N} e^{-i\boldsymbol{k}\cdot\boldsymbol{r}_n}\right\rangle. \tag{3.7}$$

which provides the structure of the system at a single moment in time. In addition to the static structure factor, the radial distribution function $g(r)$ can be calculated. The radial distribution function is similar to the static structure factor, but a key difference is that the radial distribution function is measured in real space as opposed to the spatial frequency domain (k-space) for the static structure factor. The radial distribution function is defined by the probability of finding the center of a particle in a shell at a distance r from a reference particle with thickness dr as visualized in figure 3.2. The result is divided by the number density ρ and the thickness of the cell $4\pi r^2 dr$. In practice, this radial distribution is averaged over all the particles of the system to get an accurate description of the structure.

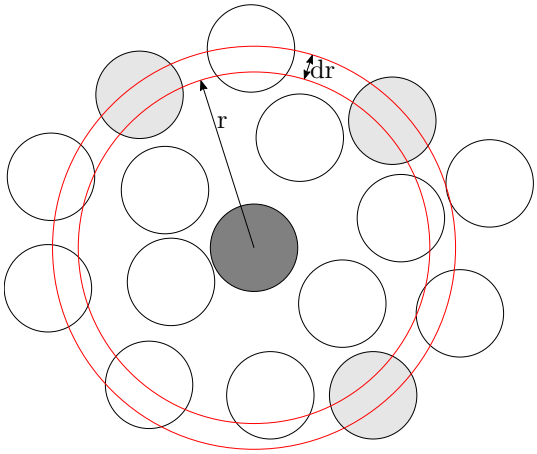

Figure 3.2: Schematic representation of the radial distribution function.

3.2 Equilibration

In order to perform measurements on the system, it is first necessary to equilibrate the system. As all simulations performed are within the canonical ensemble the number of spheres N, the volume V and the temperature T are fixed. A calculation of the energy and pressure over time is, therefore, a possibility for determining when a state is approaching equilibrium.

The energy

$$E = \sum_{i=1}^{N-1} \sum_{j=i+1}^{N} V(r_{ij}), \tag{3.8}$$

which is simply the sum of all the pairwise interaction potentials. This is due to the fact that in Monte Carlo simulations there is no explicit kinetic energy.

The pressure

$$P = \rho k_B T + \frac{1}{dV} \sum_{i=1}^{N-1} \sum_{j=i+1}^{N} \boldsymbol{F}(\boldsymbol{r}_{ij}) \cdot \boldsymbol{r}_{ij}, \tag{3.9}$$

where d is the dimensionality of the problem, which in this case is 3 [4].

A system can be falsely thought to be in equilibrium if the only metrics for determining equilibrium is the energy and the pressure. To make sure that a system is, in fact, in equilibrium one needs to check the structure over time. This can be done by looking at the radial distribution function or the static structure factor. A system that looks to be in equilibrium regarding the energy and the pressure can show signs of aging. Aging occurs when the structure ever so slightly changes over time [15], visualized in figure 3.3. So when determining if a system is in equilibrium it is important to make sure that there are no signs of aging.

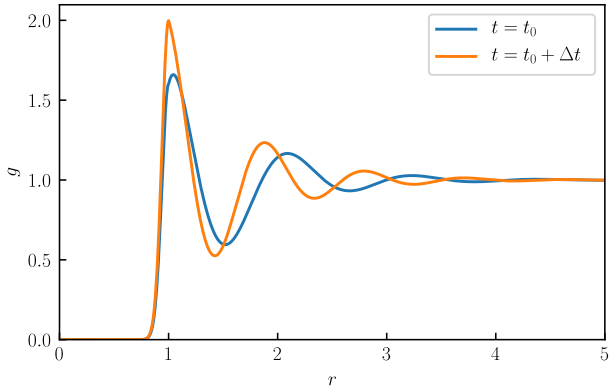

Figure 3.3: Sketch of the radial distribution function g as function of the separation distance r for two different times t_0 and $t_0 + \Delta t$, where Δt is used to illustrate some later moment in time. Due to aging the system is not yet in equilibrium, indicated by a constant structure over time. Sketch made using expression presented by Matteoli and Mansoori [16].

3.3 Verification

To make sure that the developed simulation code is correct, it is verified by reproducing literature. This is done by changing the simulation code partly to be able to compare the results to literature. First, the structure and dynamics with only conventional Monte Carlo moves is verified by reproducing the results presented by Berthier and Tarjus [17]. Next, the complete algorithm, including swap Monte Carlo moves, is verified by reproducing the dynamics published by Ninarello et al. [5].

3.3.1 Conventional Monte Carlo

The conventional Monte Carlo simulation, with $P_{\text{swap}} = 0$, is verified with the Kob-Anderson mixture [18]. The Kob-Anderson model is a binary mixture of two different sizes, a ratio of 80:20 of large to small particles [17]. Large and small particles are indicated by a subscript of A and B respectively. Interactions between two large particles, two small particles and one large with one small particle are indicated by a subscript of AA, BB and AB respectively. Lengths are given in units of the large particle σ_A. The system is modeled using the Weeks-Chandler-Andersen potential in equation A.2 with modified parameters: $\epsilon_{AA} = 1.0$, $\sigma_{AA} = 1.0$, $\epsilon_{AB} = 1.5$, $\sigma_{AB} = 0.8$, $\epsilon_{BB} = 0.5$ and $\sigma_{BB} = 0.88$ [18]. The simulations are performed with $N = 1000$ particles and a number density $\rho = 1.2$.

The structure of the Kob-Andersen mixture is visualized using the radial distribution function $g(r)$ in figure 3.4.

The structure of figure 3.4 looks equivalent to the same model studied by Berthier and Tarjus [17] shown in figure 3.5. By this note, one can conclude that the model appears to be correct for the structure using conventional Monte Carlo molecular modeling.

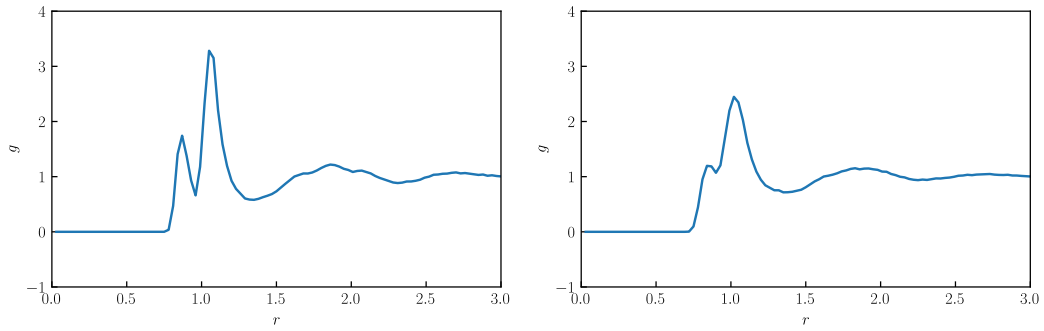

(a) T = 0.45. (b) T = 1.5.

Figure 3.4: Radial distribution function g as function of the separation distance r for different temperatures, $N = 1000$ particles are distributed using a ratio of 80:20 for large to small particles with a number density $\rho = 1.2$. The system is modeled using the WCA-potential of equation A.2.

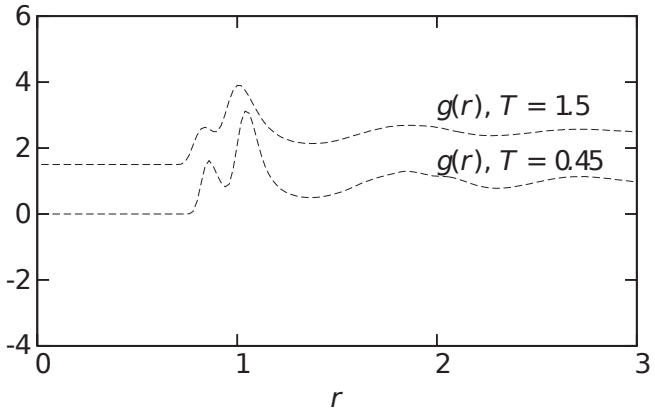

Figure 3.5: Radial distribution function g as function of the separation distance r for different temperatures. The particles are distributed using a ratio of 80:20 for large to small particles with a number density $\rho = 1.2$. The system is modeled using the WCA-potential of equation A.2. Measurements by Berthier and Tarjus [17].

The dynamics of the Kob-Andersen mixture can be described using the self intermediate scattering function $F_s(t)$ of equation 3.6 which is shown in figure 3.6.

The dynamics shown in figure 3.6 have the same behavior as the dynamics shown by Berthier and Tarjus [17] shown in figure 3.7. However, an important difference is the time-scales involved. As discussed Monte Carlo simulation do not have an explicit time in contrast to Molecular Dynamics, which was used by Berthier and Tarjus [17] in figure 3.7. Taking both considerations into account it can reasonably be assumed that the model is correct for describing dynamics using conventional Monte Carlo molecular modeling.

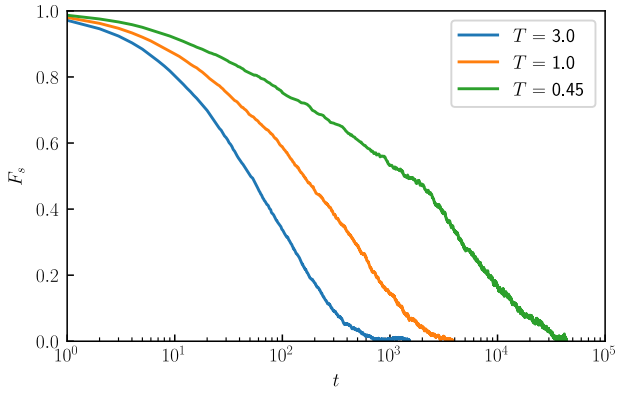

Figure 3.6: Self intermediate scattering function F_s as function of the time t for different temperatures. $N = 1000$ particles are distributed using a ratio of 80:20 for large to small particles with a number density $\rho = 1.2$. The system is modeled using the WCA-potential of equation A.2.

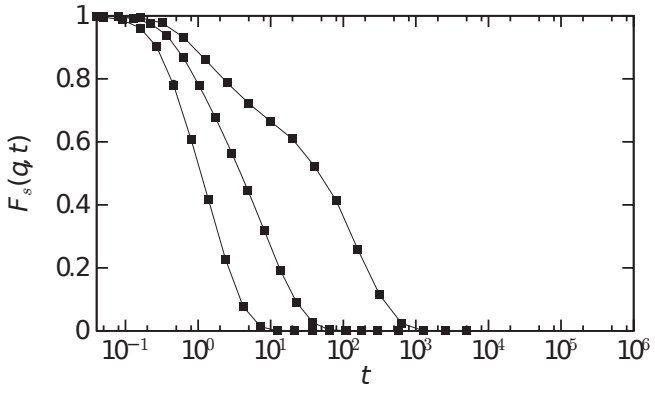

Figure 3.7: Self intermediate scattering function F_s as function of the time t for different temperatures. The temperatures are $T = 3.0, 1.0, 0.45$ from left to right. The particles are distributed using a ratio of 80:20 for large to small particles with a number density $\rho = 1.2$. The system is modeled using the WCA-potential of equation A.2. Measurements by Berthier and Tarjus [17].

3.3.2 Swap Monte Carlo

To verify the model with the swap Monte Carlo algorithm the dynamics are compared to Ninarello et al. [5]. The system with a number density $\rho = 1.0$ uses the soft repulsive pair potential of equation 2.12 with a softness $n = 12$ and a cross diameter calculated using equation 2.18 with a nonadditivity parameter $\alpha = 0.2$. The particle mixture with $N = 1000$ particles is continuous polydisperse with a distribution as in equation 2.19 using a diameter ratio $\sigma_{\max}/\sigma_{\min} = 2.219$. In figure 3.8 the self intermediate scattering function $F_s(t)$, according to equation 3.6, is shown for various temperatures.

The dynamics shown in figure 3.8 look similar to the same system studied by Ninarello et al. [5] shown in figure 3.9. As mentioned before, the time t can not directly be compared to the reference study. This is in this case not because of the different molecular modeling method, which is both Monte Carlo, but because in the reference study it is not documented which maximum translation step size l is used. This strongly affects the Monte Carlo translation step acceptance rate, which is directly related to the dynamics. In addition, the value of the self intermediate scattering function should be averaged over multiple runs to get a more accurate and smooth result. There is also more computation time needed before all systems reach $F_s = 0$ and the full behavior can be known. However, the measurements shown signs of plateauing for temperatures $T = 0.075$ and $T = 0.062$ similar to the reference study [5], shown in figure 3.9. Because of this, it is concluded that the model behaves properly for systems using the swap Monte Carlo algorithm.

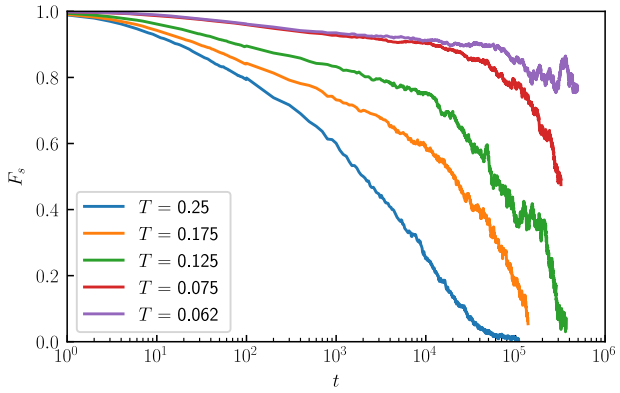

Figure 3.8: Self intermediate scattering function F_s as function of the time t for different temperatures. The system used is a continuous polydisperse mixture of $N = 1000$ particles distributed using equation 2.19 with a diameter ratio $\sigma_{\max}/\sigma_{\min} = 2.219$ and a number density $\rho = 1.0$. The interaction potential is the soft repulsive pair potential described in equation 2.12 with a softness $n = 12$ and nonadditivity $\alpha = 0.2$.

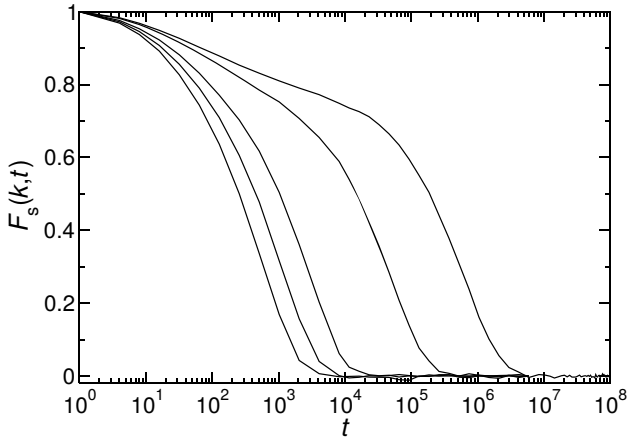

Figure 3.9: Self intermediate scattering function F_s as function of the time t for different temperatures. The temperatures are $T = 0.25, 0.175, 0.125, 0.075, 0.062$ from left to right. The system used is a continuous polydisperse mixture distributed using equation 2.19 with a diameter ratio $\sigma_{\max}/\sigma_{\min} = 2.219$ and a number density $\rho = 1.0$. The interaction potential is the soft repulsive pair potential described in equation 2.12 with a softness $n = 12$ and nonadditivity $\alpha = 0.2$. Measurements by Ninarello et al. [5].

Chapter 4

Results and discussion

In section 4.1 the results are presented for the continuous polydisperse mixture, an infinite number of possible particle diameters, in the context of showing the effects of the swap Monte Carlo moves on the structure and dynamics of supercooled liquids. In section 4.2 the results are presented for the discrete polydisperse mixture to see how many species such a system should contain to have similar dynamics and structure as a continuous polydisperse system.

4.1 Continuous polydisperse mixture

The system used is a continuous polydisperse mixture of $N = 1000$ particles distributed using equation 2.19 with a diameter ratio $\sigma_{\max}/\sigma_{\min} = 2.219$ and a number density $\rho = 1.0$. The interaction potential is the soft repulsive pair potential described in equation 2.12 with a softness $n = 12$ and nonadditivity $\alpha = 0.2$.

To calculate the most optimal swap probability P_{swap} for increasing the thermalization speed, the continuous polydisperse system following the distribution in equation 2.19 is simulated for different swap probabilities. The results are graphed in figure 4.1. Figure 4.1 shows that the structural relaxation time is the lowest, therefore the most optimal, over a fairly large range of swap probabilities $P_{\text{swap}} = 0.2$ until $P_{\text{swap}} = 0.5$. As a Monte Carlo simulations with $P_{\text{swap}} = 1$ take, in terms of CPU time, about 50% longer than with $P_{\text{swap}} = 0$ and similar to Ninarello et al. [5] for $P_{\text{swap}} = 0.2$ about 20% longer, $P_{\text{swap}} = 0.2$ is found to be optimal and is used for further simulations. However, it should be noted that even for very small swap probabilities there is a huge decrease in relaxation time.

Figure 4.2 shows the acceptance rates of swap and translation Monte Carlo moves for varying temperature T. For $T \to \infty$ the acceptance rate will increase to a constant value. On top of this, simulations show that swap and translation acceptance ratios do not change as function of the swap probability. Possible improvements to increase the translation acceptance rate would be to decrease the maximum translation step l. This makes it less likely that a move is proposed which is energetically very unfavorable. Next, it is possible to make the maximum translation step in units of the chosen particle diameter, such that a small particle cannot move as much in one Monte Carlo sweep as a large particle. To further tweak the translation Monte Carlo move to speed up the simulation time one could introduce a variable maximum translation step which tries to get the translation acceptance within a certain range, say 30-60% by checking every few iterations what the acceptance rate was and increasing or decreasing the maximum translation step by a few percents for the next batch of iterations [19]. However, it should be noted that this variable step size can only be used for equilibration or when measuring structure, but is not to be used when measuring dynamics as this would change the time intervals between every iteration.

As shown in figure 4.3 the structural relaxation time τ_α for the system with swap moves

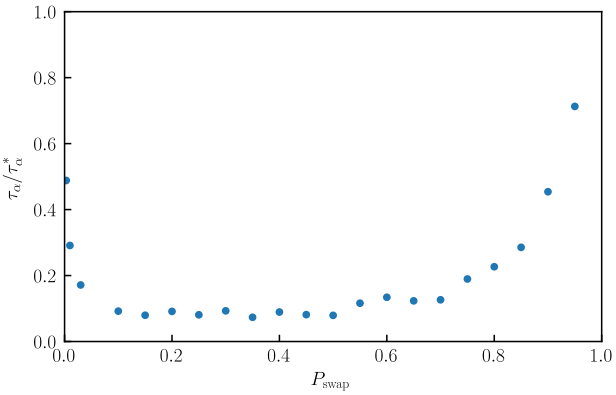

Figure 4.1: Structural relaxation time τ_α as function of the swap probability P_{swap} normalized by the structural relaxation time with a swap probability $P_{\text{swap}} = 0$ denoted by τ_α^* for a temperature $T = 0.25$. The system used is a continuous polydisperse mixture of $N = 1000$ particles distributed using equation 2.19 with a diameter ratio $\sigma_{\text{max}}/\sigma_{\text{min}} = 2.219$ and a number density $\rho = 1.0$. The interaction potential is the soft repulsive pair potential described in equation 2.12 with a softness $n = 12$ and nonadditivity $\alpha = 0.2$.

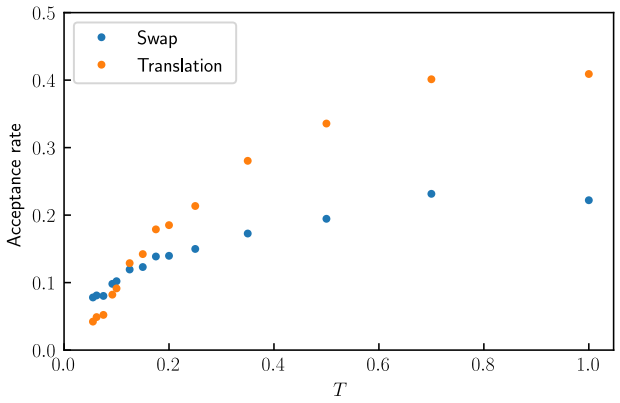

Figure 4.2: Monte Carlo acceptance rates as function of the temperature T using a swap probability $P_{\text{swap}} = 0.2$. The system used is a continuous polydisperse mixture of $N = 1000$ particles distributed using equation 2.19 with a diameter ratio $\sigma_{\text{max}}/\sigma_{\text{min}} = 2.219$ and a number density $\rho = 1.0$. The interaction potential is the soft repulsive pair potential described in equation 2.12 with a softness $n = 12$ and nonadditivity $\alpha = 0.2$.

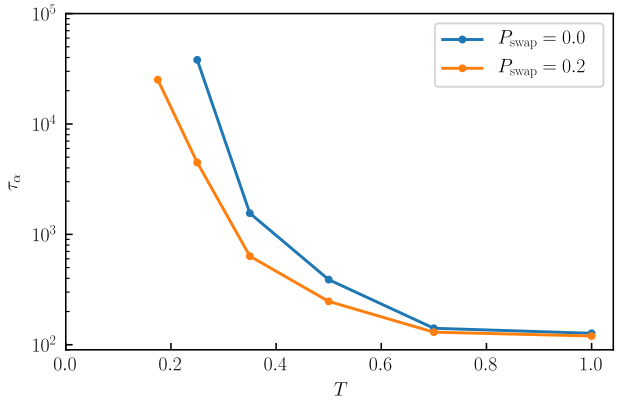

Figure 4.3: Structural relaxation time τ_α as function of the temperature T for swap probabilities $P_{\text{swap}} = 0.0, 0.2$. The system used is a continuous polydisperse mixture of $N = 1000$ particles distributed using equation 2.19 with a diameter ratio $\sigma_{\text{max}}/\sigma_{\text{min}} = 2.219$ and a number density $\rho = 1.0$. The interaction potential is the soft repulsive pair potential described in equation 2.12 with a softness $n = 12$ and nonadditivity $\alpha = 0.2$.

already shows an order of magnitude improvements for a temperature $T = 0.25$. Extrapolating the data for $P_{\text{swap}} = 0.0$ in figure 4.3 to a temperature of 0.2 gives a difference of 2 order of magnitudes with respect to the data obtained for $P_{\text{swap}} = 0.2$. Simulations for lower temperatures and thereby increasingly longer computation time have to be done to show the dramatic speedup of 10 orders of magnitude calculated using extrapolation by Ninarello et al. [5].

In simulations from the same state to a lower temperature there can not be found a significant difference in the equilibrium energy or pressure when introducing swap moves on top of the conventional translation moves. Figure 4.4 shows that, in addition to no significant difference in equilibrium energy or pressure, there is also not a notable difference in structure. The slight mismatch in figure 4.4 can be caused by noise which could be resolved by averaging over even more timesteps.

In summary, swap moves seem to speed up the relaxation time greatly. For a temperature $T = 1.0$ there is hardly any different but for lower a temperature $T = 0.25$ an order of magnitude in speedup is found. On top of that, for even lower temperatures, the swap dynamics have shown to speed up the relaxation time even further. Comparing simulations using conventional Monte Carlo translation with simulations that also have the possibility to perform swap moves shows that there is not a significant difference between the energy, pressure and the structure of both mixtures.

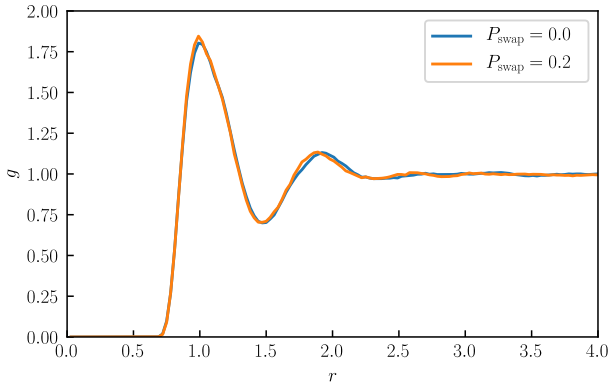

Figure 4.4: Radial distribution function g as function of the separation distance r for swap probabilities $P_{\text{swap}} = 0.0, 0.2$ at temperature $T = 0.25$. The system used is a continuous polydisperse mixture of $N = 1000$ particles distributed using equation 2.19 with a diameter ratio $\sigma_{\text{max}}/\sigma_{\text{min}} = 2.219$ and a number density $\rho = 1.0$. The interaction potential is the soft repulsive pair potential described in equation 2.12 with a softness $n = 12$ and nonadditivity $\alpha = 0.2$.

4.2 Discrete polydisperse mixture

A continuous polydisperse mixture is theoretical the most optimal mixture for increasing the acceptance of swap Monte Carlo moves, but is impossible to use in combination with Mode-Coupling Theory as explained in chapter 1. Therefore, the goal is to find an optimum number of species to approximate the behavior seen for a continuous polydisperse mixture. The system used is a discrete polydisperse mixture of $N = 1000$ particles distributed using equation 2.19 with a diameter ratio $\sigma_{\text{max}}/\sigma_{\text{min}} = 2.219$ and a number density $\rho = 1.0$. The interaction potential is the soft repulsive pair potential described in equation 2.12 with a softness $n = 12$ and nonadditivity $\alpha = 0.2$.

Figure 4.5 shows for systems with $P_{\text{swap}} = 0.2$ and the number of component around $N_s = 10, 20$ the structural relaxation time is already very close to the relaxation time of a continuous polydisperse system τ_α^∞. The relaxation time for discrete polydisperse systems with $P_{\text{swap}} = 0.0$ and varying the number of species N_s stays equal to the relaxation time of a continuous polydisperse system. Averaging the self intermediate scattering function F_s over a large number of simulations would decrease the fluctuations in structural relaxation time τ_α but due to time and storage size constraints, this is being skipped for this work. In figure 4.6 the Monte Carlo acceptance rate is visualized as a function of the number of components N_s. The acceptance rate of the swap Monte Carlo moves is vanishingly small for $N_s < 7$. For $N_s \geq 7$ the acceptance rates for the swap moves increases a lot, while the acceptance rate of the translation moves does not change significantly. This indicates that the speedup shown in figure 4.5 is entirely due to the fact that swap moves come into effect.

In figure 4.7 a detailed view of the relaxation time as function of the temperature is given for $N_s = 10$ and $N_s = 20$. The relaxation time speedups using swap Monte Carlo moves in figure 4.7 is very similar to the the speedups for the continuous polydisperse system in figure 4.3.

Figure 4.8 shows that the optimal swap probability for $N_s = 10$ and $N_s = 20$ is identical to the continuous polydisperse mixture as concluded from figure 4.1.

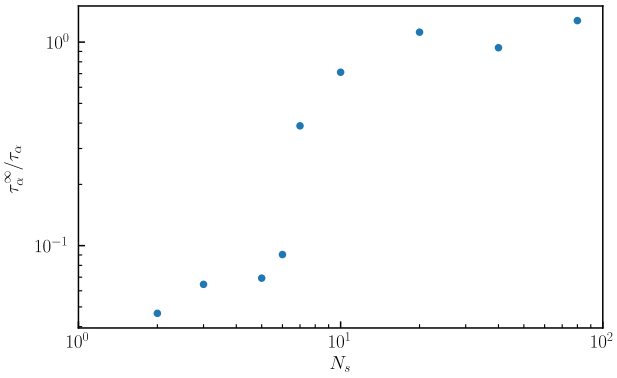

Figure 4.5: Inverse structural relaxation time $1/\tau_\alpha$ as function of the number of species N_s multiplied with the structural relaxation time for a continuous polydisperse system τ_α^∞ for swap probability $P_{\text{swap}} = 0.2$ at temperature $T = 0.25$. The system used is a discrete polydisperse mixture of $N = 1000$ particles distributed using equation 2.19 with a diameter ratio $\sigma_{\text{max}}/\sigma_{\text{min}} = 2.219$ and a number density $\rho = 1.0$. The interaction potential is the soft repulsive pair potential described in equation 2.12 with a softness $n = 12$ and nonadditivity $\alpha = 0.2$.

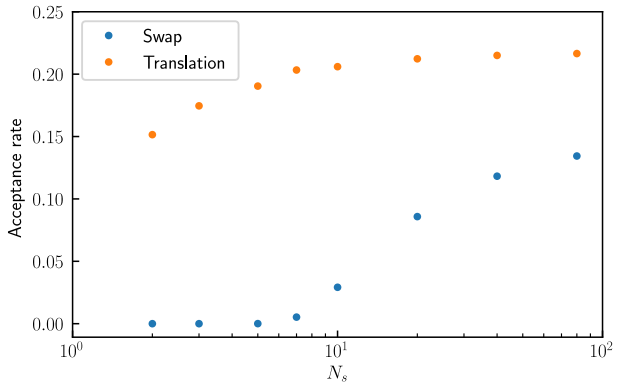

Figure 4.6: Monte Carlo acceptance rates as function of the number of species N_s at temperature $T = 0.25$ using a swap probability $P_{\text{swap}} = 0.2$. The system used is a discrete polydisperse mixture of $N = 1000$ particles distributed using equation 2.19 with a diameter ratio $\sigma_{\text{max}}/\sigma_{\text{min}} = 2.219$ and a number density $\rho = 1.0$. The interaction potential is the soft repulsive pair potential described in equation 2.12 with a softness $n = 12$ and nonadditivity $\alpha = 0.2$.

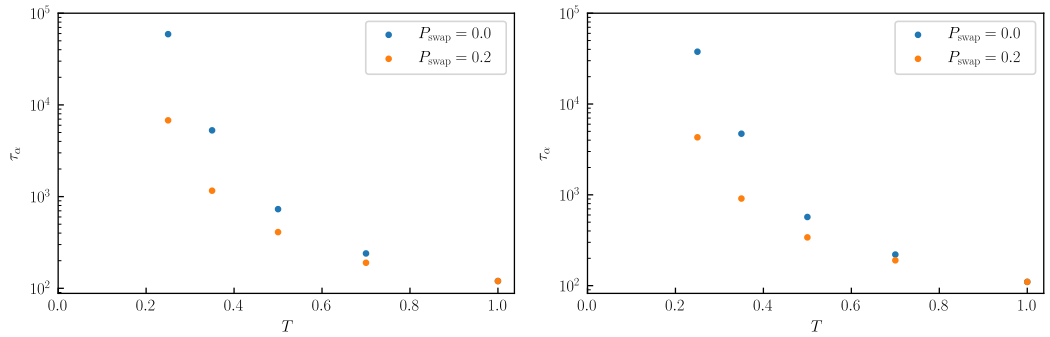

(a) Number of species $N_s = 10$.

(b) Number of species $N_s = 20$.

Figure 4.7: Structural relaxation time τ_α as function of the temperature T for for swap probability $P_{\text{swap}} = 0.0, 0.2$ for a temperature $T = 0.25$. The system used is a discrete polydisperse mixture of $N = 1000$ particles distributed using equation 2.19 with a diameter ratio $\sigma_{\max}/\sigma_{\min} = 2.219$ and a number density $\rho = 1.0$. The interaction potential is the soft repulsive pair potential described in equation 2.12 with a softness $n = 12$ and nonadditivity $\alpha = 0.2$.

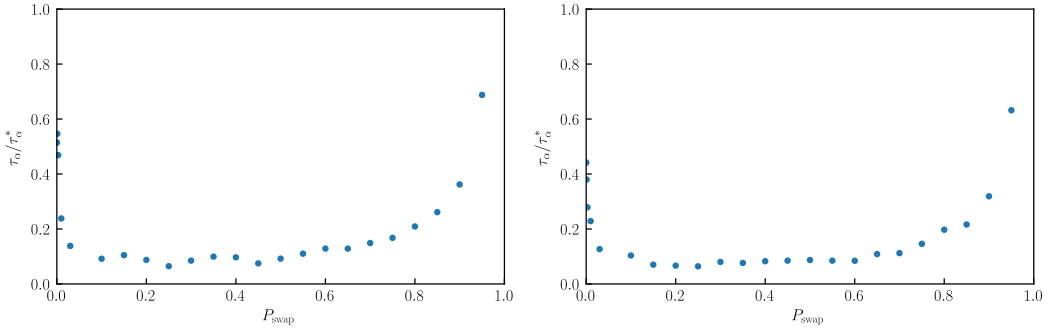

(a) Number of species $N_s = 10$.

(b) Number of species $N_s = 20$.

Figure 4.8: Structural relaxation time τ_α as function of the swap probability P_{swap} normalized by the structural relaxation time with a swap probability $P_{\text{swap}} = 0$ denoted by τ_α^* for a temperature $T = 0.25$. The system used is a discrete polydisperse mixture of $N = 1000$ particles distributed using equation 2.19 with a diameter ratio $\sigma_{\max}/\sigma_{\min} = 2.219$ and a number density $\rho = 1.0$. The interaction potential is the soft repulsive pair potential described in equation 2.12 with a softness $n = 12$ and nonadditivity $\alpha = 0.2$.

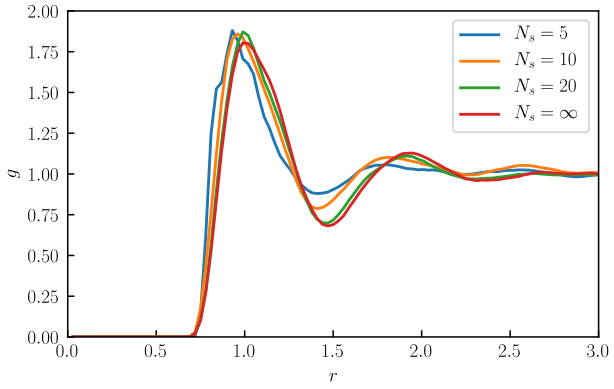

Figure 4.9: Radial distribution function g as function of the separation distance r for different number of species N_s, including for a continuous polydisperse mixture indicated by $N_s = \infty$, at a swap probability $P_{\text{swap}} = 0.0$ and temperature $T = 0.25$. The system used is a discrete polydisperse mixture of $N = 1000$ particles distributed using equation 2.19 with a diameter ratio $\sigma_{\text{max}}/\sigma_{\text{min}} = 2.219$ and a number density $\rho = 1.0$. The interaction potential is the soft repulsive pair potential described in equation 2.12 with a softness $n = 12$ and nonadditivity $\alpha = 0.2$.

In figure 4.9 the structure of the system for different number of species N_s is shown in contrast to structure for a continuous polydisperse mixture. The structure shows that for $N_s = 10$, in contrast to $N_s = 20$, the structure still appears to be different from the continuous polydisperse mixture.

Altogether this means that to have similar dynamics as a continuous polydisperse system one needs a minimum of 10 species, while for the structure to be similar around 20 species is needed.

Chapter 5

Conclusion

With the aim in mind of simulating very low-temperature supercooled liquid, we studied the effect of Monte Carlo swaps. In general, we were discussing the idea that with Monte Carlo swaps we can simulate lower temperature supercooled liquids, but in this particular work simulations were done on nonadditive particles, with various degrees of size distribution and interacting using a soft repulsive pair potential to show the effects of Monte Carlo swaps in speeding up the structural relaxation of supercooled liquids.

As discussed the workings of the swap Monte Carlo algorithm are optimal for a continuous polydisperse system. For a system of 1000 particles an ideal swap probability $P_{\text{swap}} = 0.2$ is found which result in the strongest decrease in relaxation time while taking CPU time into account. The performance of the Monte Carlo simulation is analyzed using the move acceptance rates as a function of the temperature, which shows that the acceptance rate increases for higher temperature as expected when using Boltzmann probabilities to sample the system. The relaxation time decreases when introducing particle swaps is larger for lower temperatures. For a temperature of 0.25 this speedup in dynamics is already an order of magnitude and even more for lower temperatures. It is shown that the structure of systems with swap moves is identical to the structure of a system without swap moves.

As existing theories of glass forming are very difficult, if not impossible, to generalize to an infinite amount of species the quest was born to find a number of species which approximates the continuous polydispersity, such that the similar decrease in relaxation time, using swap Monte Carlo, can be found without using an infinite number of species. The relaxation time as a function of the number of species is calculated and compared to the relaxation time for a continuous polydisperse system. To get an approximately similar relaxation time as the continuous polydisperse system one needs to use a multicomponent mixture of around 10 to 20 species. The reason for this is further analyzed by measuring the acceptance rates of the Monte Carlo moves as a function of the number of components. For less than 7 species at a low temperature, the swap acceptance rate is approximately zero. This results in an increase in relaxation time as every proposed swap move gets rejected. The relaxation time as a function of the temperature for 10 and 20 species is compared to the continuous polydisperse mixture and looks very similar, having an order of magnitude speedup in dynamics for a temperature of 0.25. The swap probability optimization as performed for the continuous polydisperse mixture is repeated for the discretized polydisperse mixture with 10 and 20 components from which a similar value is found, compared to an infinite number of species. When comparing the structure for the previously mentioned systems, the structure of the 20 component and the continuous polydisperse mixture are almost indistinguishable.

Swap Monte Carlo has shown to be a strong improvement over current methods bringing us one step closer to discover the mysteries of the glass formation.

Bibliography

[1] P.W. Anderson. Through the Glass Lightly. *Science*, 267(5204):1615–1616, 1995.

[2] E.D. Zanotto. Do cathedral glasses flow? *American Journal of Physics*, 66(5):392–395, 2005.

[3] L.M.C. Janssen. Mode-Coupling Theory of the Glass Transition: A Primer. *Frontiers in Physics*, 6:97, 2018.

[4] D. Frenkel and B. Smit. *Understanding molecular simulation: from algorithms to applications*. Academic Press, 2002.

[5] A. Ninarello, L. Berthier, and D. Coslovich. Models and algorithms for the next generation of glass transition studies. *Physical Review X*, 7(2):1–22, 2017.

[6] C.P. Royall, F. Turci, S. Tatsumi, J. Russo, and J. Robinson. The race to the bottom: approaching the ideal glass? *Journal of Physics: Condensed Matter*, 30(36):363001, 9 2018.

[7] T.S. Grigera and G. Parisi. Fast Monte Carlo algorithm for supercooled soft spheres. *Physical Review E - Statistical Physics, Plasmas, Fluids, and Related Interdisciplinary Topics*, 63(4):63–66, 2001.

[8] F. Weysser, A.M. Puertas, M. Fuchs, and T. Voigtmann. Structural relaxation of polydisperse hard spheres: Comparison of the mode-coupling theory to a Langevin dynamics simulation. *Physical Review E - Statistical, Nonlinear, and Soft Matter Physics*, 82(1):1–21, 2010.

[9] N. Metropolis, A.W. Rosenbluth, M.N. Rosenbluth, A.H. Teller, and E. Teller. Equation of state calculations by fast computing machines. *The Journal of Chemical Physics*, 21(6):1087–1092, 1953.

[10] K. Binder and D.W. Heermann. *Monte Carlo Simulation in Statistical Physics*. Graduate Texts in Physics. Springer Berlin Heidelberg, Berlin, Heidelberg, 2010.

[11] H. Müller-Krumbhaar and K. Binder. Dynamic properties of the Monte Carlo method in statistical mechanics. *Journal of Statistical Physics*, 8(1):1–24, 1973.

[12] J.D. Weeks, D. Chandler, and H.C. Andersen. Role of repulsive forces in determining the equilibrium structure of simple liquids. *The Journal of Chemical Physics*, 54(12):5237–5247, 1971.

[13] M.P. Allen and D.J. Tildesley. *Computer Simulation of Liquids*. Oxford Science. Clarendon Press, 1989.

[14] K. Zhang. On the Concept of Static Structure Factor. Technical report, Department of Chemical Engineering, Columbia University, 2016.

[15] D. Mukherji and M.H. Müser. Glassy dynamics, aging in mobility, and structural relaxation of strongly adsorbed polymer films: Corrugation or confinement? *Macromolecules*, 40(5):1754–1762, 2007.

[16] E. Matteoli and G. Ali Mansoori. A simple expression for radial distribution functions of pure fluids and mixtures. *The Journal of Chemical Physics*, 103(11):4672–4677, 1995.

[17] L. Berthier and G. Tarjus. The role of attractive forces in viscous liquids. *Journal of Chemical Physics*, 134(21), 2011.

[18] W. Kob and H.C. Andersen. Scaling behavior in the dynamics of a supercooled Lennard-Jones mixture. *Il Nuovo Cimento D*, 16(8):1291–1295, 8 1994.

[19] R.H. Swendsen. How the maximum step size in Monte Carlo simulations should be adjusted. *Physics Procedia*, 15(12-2011):81–86, 2011.

Appendix A

Weeks-Chandler-Andersen potential

The interaction between particles i and j is modelled via the Lennard-Jones potential

$$V_{LJ}(r_{ij}) = 4\epsilon \left[\left(\frac{\sigma_{ij}}{r_{ij}} \right)^{12} - \left(\frac{\sigma_{ij}}{r_{ij}} \right)^{6} \right], \tag{A.1}$$

where ϵ is a measure of interaction between the particles i and j. σ_{ij} is the diameter of a hard sphere or otherwise known as the summed van der Waals radius of particles i and j. r_{ij} is the Euclidean distance between the centers of particle i and j.

In 1971 Weeks, Chandler and Anderson introduced a modified version of the Lennard-Jones potential in which the repulsive property is isolated [12]. By truncating and shifting at the minimum giving a cut-off distance $r_{cut} = 2^{1/6}$ the continuity of the Weeks-Chandler-Andersen potential and its first derivative is ensured. Up until the cut-off distance, the derivative is always negative, indicating a repulsive interaction. The Weeks, Chandler and Anderson potential, from here on called the WCA-potential,

$$V_{WCA}(r_{ij}) = \begin{cases} V_{LJ}(r_{ij}) + \epsilon & \text{if } r < 2^{1/6}\sigma \\ 0 & \text{if } r \geq 2^{1/6}\sigma, \end{cases} \tag{A.2}$$

which is visualized in figure 2.3. The force due to the WCA potential

$$F_{WCA,x}(x, r_{ij}) = \begin{cases} 24\epsilon \left[\frac{2\sigma^{12}}{r^{14}} - \frac{\sigma^6}{r^8} \right] x & \text{if } r < 2^{1/6}\sigma \\ 0 & \text{if } r \geq 2^{1/6}\sigma, \end{cases} \tag{A.3}$$

where x is the one dimensional distance in the x-direction. Similarly, the can force be computed for the y and z-direction.

Appendix B

Simulation code

Getting started

The simulation is written in the C++ programming language. The code is openly available on GitHub via `https://github.com/GillesBonne/swap_mc`. The executable can be build by using the MAKEFILE provided in the repository.

Before building it is important to provide some configuration preferences in the code itself. The available options, to be changed in /SRC/SYSTEM.H, are:

- WCA potential (equation A.2) or soft repulsive pair potential (equation 2.12).
- Continuous or discretized polydispersity.
- Kob-Anderson proposed interaction parameters [17].
- Nonadditivity.

If the option of a discretized polydispersity is turned on, one needs to specify the number of species in /SRC/SYSTEM.CPP.

Performing a simulation

Before performing a simulation the CONFIG.TXT file needs to be adapted to use specific simulation parameters. When running the simulation it is possible to provide some command line arguments:

- None.
- Number of iterations before sampling.
- Simulation identification.
- Simulation identification of a previous simulation, such that the simulation can continue from the state where the previous simulation has stopped.

Interpreting the output

The simulation samples the energy, pressure and Monte Carlo acceptance ratios on a logarithmic scale (iteration number: 1,2,...,9,10,20,...,90,100,200,...). The particle configurations are sampled every set number of iterations. The code in /PYTHON/ is used to visualize all this saved information.

Supplementary Mathematica code

In the folder /MATHEMATICA/ additional Mathematica files are supplemented. These calculate $\sigma_{\max}$ and $\sigma_{\min}$ for continuous and discretized polydisperse systems. In addition, the calculation of the coefficients of the soft repulsive pair potential is added.